Journal of Alloys and Compounds 509 (2011) 1355–1359

Contents lists available at ScienceDirect

Journal of Alloys and Compounds

journal homepage: www.elsevier.com/locate/jallcom

$ZnWO_4:Eu^{3+}$ nanorods: A potential tunable white light-emitting phosphors

X.P. Chen, F. Xiao, S. Ye, X.Y. Huang, G.P. Dong, Q.Y. Zhang*

MOE Key Lab of Specially Functional Materials and Institute of Optical Communication Materials, South China University of Technology, #381, Wushan Road, Guangzhou 510641, PR China

ARTICLE INFO

Article history:
Received 2 July 2010
Received in revised form 6 October 2010
Accepted 17 October 2010
Available online 23 October 2010

PACS:
42.50.Fx
32.70.Cs
33.50.Hv
78.67.−n

Keywords:
Phosphors
White light-emitting diodes
Hydrothermal synthesis
$ZnWO_4:Eu^{3+}$ nanorod
Energy transfer

ABSTRACT

One-dimensional $ZnWO_4:Eu^{3+}$ nanorods with excellent photoluminescence (PL) properties were prepared by a facile template-free hydrothermal route. The products were characterized by X-ray diffraction (XRD), transmission electron microscopy (TEM) as well as PL spectra. The results show that tunable color from blue through white to orange could be obtained by adjusting the doping concentration of Eu^{3+}. It is notable that white light with CIE chromaticity coordinates of $x = 0.32$, $y = 0.30$ and the correlative color temperature of 5919 K could be observed by combining the broad blue-green emission band assigned to the charge transfer transition of tungstate group with red emission from Eu^{3+}, upon the excitation of ultraviolet radiation.

© 2010 Elsevier B.V. All rights reserved.

1. Introduction

One-dimensional lanthanide-doped nanomaterials have attracted extensive attention in luminescence devices, displays, biolabeling and other functional materials owing to their electronic, optical and chemical properties originated from the 4*f* shell of rare earth ions [1–4]. Especially for high-performance Eu^{3+}-doped phosphor, this is a key component for tri-color luminescence in various devices to realize white light. Phosphors converted white light-emitting diodes (pc-WLEDs) are considered as the next generation solid state lighting, the commercial available pc-WLEDs are mostly fabricated by combining blue LED with a yellow emitting phosphor (YAG:Ce) [5,6]. However, the lack of red emitting component results in low color rendering index (CRI) [7]. The commonly alternative way is to employ an ultraviolet (UV) LED chip as the excitation light source with different color phosphors [8,9]. Furthermore, a kind of single-phased white-emitting phosphor has triggered active research efforts recently, which includes an appropriate host lattice with singly doping Eu^{3+} ion [10–12]. All their principles can be summarized to the abundant Eu^{3+} emissions which yield the blue and green emissions from the higher ^5D_J levels ($^5D_1$, $^5D_2$, and $^5D_3$) and the red emission from the $^5D_0$ level to ^7F_J ($J = 0$–4) of Eu^{3+} simultaneously, then the combination of comparable multi-color emissions produces the white light.

Zinc tungstate ($ZnWO_4$) is well-known for its traditional applications in optical fields such as X-ray scintillator, photoanode and solid state laser host [13]. As a self-activating phosphor, $ZnWO_4$ exhibits a broad, intrinsic blue-green emission band under deep UV excitation [14]. The well-researched deep UV LED based on AlGaN semiconductor can perfectly provide excitation wavelength in the range of 280–315 nm [15,16]. Therefore, considering the high chemical stability, short decay time and non-toxicity of tungstate, $ZnWO_4:Eu^{3+}$ may be an ideal candidate for white light source by combining the red emission from Eu^{3+} with the blue-green emission from tungstate group [17]. $ZnWO_4$-based material can be prepared by various traditional methods [18,19], however, some treatments may increase the size of the product regardless of the shape. Controlled synthesis of well-defined crystals is of extraordinary importance because the electronic structure, bonding and surface energy are directly related to their surface morphology [20]. Hydrothermal method is a promising synthetic route, which can be better controlled from the molecular precursor to the reaction parameters, such as the reaction time and temperature, to give highly pure and homogeneous materials [11,21–23].

Herein, the main objective of this work is to carry out a detailed study on synthesis and PL properties of the $ZnWO_4:Eu^{3+}$ nanorods, and to examine their suitability as potential white light-emitting

* Corresponding author. Tel.: +86 20 87113681; fax: +86 20 87114204.
E-mail address: qyzhang@scut.edu.c (Q.Y. Zhang).

0925-8388/$ – see front matter © 2010 Elsevier B.V. All rights reserved.
doi:10.1016/j.jallcom.2010.10.061

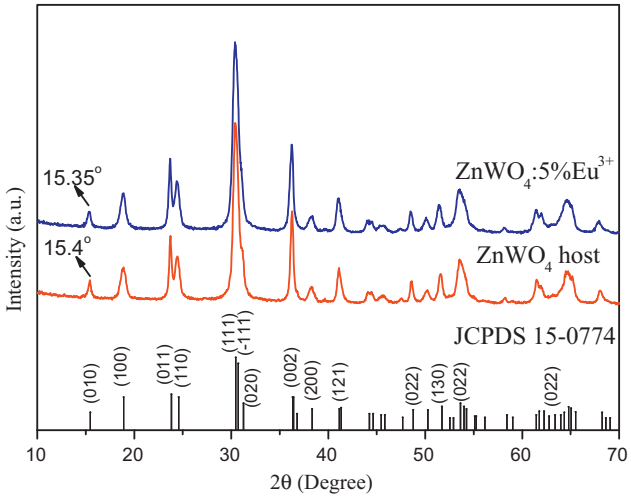

Fig. 1. XRD patterns of $ZnWO_4$ and $ZnWO_4$:5% Eu^{3+} synthesized hydrothermally at 180 °C for 12 h with pH = 6. The peaks of the main crystal phase are consistent well with monoclinic $ZnWO_4$ (JCPDS: 15-0774).

phosphors for pc-WLEDs. A tunable emission color especially a nearly ideal white light under UV wavelength radiation was realized by adjusting the doping concentration of Eu^{3+}.

2. Experimental details

All the reagents were analytical grade and used without further purification. Take $ZnWO_4$:5% Eu^{3+} as an example. 4.75 mmol (1.413 g) $Zn(NO_3)_2{\cdot}6H_2O$ was dissolved in 5 mL distilled water, 5 mL (0.05 M) $Eu(NO_3)_3$ aqueous solution was added with vigorous stirring to form a transparent solution. Then 10 mL (0.5 M) Na_2WO_4 aqueous solution was dropwise added into the mixed solution to form white suspension. The pH value of the reaction system was adjusted using ammonia solution (27 wt.%). After magnetic stirring for 30 min, the precursor suspension was transferred into a 50 mL Teflon-lined stainless autoclave, filled up to 80% of its capacity, sealed and maintained at 180 °C for 12 h in an electrical oven. After air-cooled, the precipitates were centrifuged several times with distilled water and absolute ethanol, then dried at 80 °C for 8 h. $ZnWO_4$:x Eu^{3+} (x = 0, 0.1, 0.5, 1, 2, 3 mol.%) were obtained by the similar process. The products were characterized by various tests including X-ray diffraction (XRD, Philips PW1830 with Cu K_α irradiation at 40 kV and 40 mA), transmission electron microscopy (TEM, JEM-2010), and PL spectroscopy (Jobin-Yvon Triax 320 with 450 W xenon lamp as the excitation source).

3. Results and discussion

Fig. 1 represents the XRD patterns of the $ZnWO_4$ and $ZnWO_4$:5% Eu^{3+} synthesized hydrothermally at 180 °C for 12 h with pH = 6, respectively. As detected by XRD, all diffraction peaks can be readily indexed to the pure monoclinic $ZnWO_4$ (JCPDS: 15-0774) with space group of $P2/c$. No additional peaks of other phases have been found, indicating that the existence of Eu^{3+} did not significantly influence the phase and crystallization of the products. The ionic radius of Eu^{3+} (0.95 Å) is slightly larger than that of Zn^{2+} (0.74 Å), but much larger than that of W^{6+} (0.62 Å) in 6-fold coordination, so Eu^{3+} prefers to locating in Zn^{2+} sites without inversion center. As the amount of Eu^{3+} increases, it is observed that the corresponding XRD peaks move to lower degree.

A typical TEM image of the synthesized $ZnWO_4$:Eu^{3+} nanorods is shown in Fig. 2(a), indicating that the product mainly consists of a large quantity of straight nanorods with smooth surface and an uniform diameter of several tens of nanometers. The inset in Fig. 2(a) shows the selected-area electron diffraction (SADE) pattern for a single nanorod. As depicted in Fig. 2(b), the high resolution TEM (HRTEM) image of the corresponding single nanorod reveals that the spacing of the two adjacent fringes is 2.46 Å, which matches well with the interplanar spacing of (0 0 2) and suggests the growth direction is perpendicular to the (0 0 2) plane (indicated with an arrow). The clear lattice fringes without dislocation further confirm the singly crystal structure of $ZnWO_4$ nanorods. The energy dispersive spectrometry (EDS) pattern of the $ZnWO_4$:Eu^{3+} is shown in the inset of Fig. 2(c). The presence of Zn, W, O and Eu is confirmed by EDS, and no other element except Au existing for the coating of the measurement. $ZnWO_4$ has a wolframite-type crystalline structure, in this structure, each W is surrounded by four nearest oxygen ions and two more distant ones in approximately octahedral coordination to form a WO_6^{2-} molecular complex and each octahedron shares two corners with its neighbors as shown in Fig. 2(d) [24,25].

PL excitation (PLE) and emission (PL) spectra of $ZnWO_4$ host lattice and $ZnWO_4$:5% Eu^{3+} nanorods are displayed in Fig. 3. For $ZnWO_4$ host lattice, two notable broad bands extending from 260 to 320 nm with peak wavelength at 282 and 309 nm can be detected when monitored at 466 nm (line a), which are both assigned to the transition from O → W ligand to metal charge transfer (LMCT). For the doped case, the PLE spectrum (line b) is composed of both LMCT and the characteristic sharp lines of Eu^{3+} peaking at 362, 384, 394, and 415 nm which correspond to the transitions of $^7F_0 \rightarrow {}^5D_4$, $^7F_0 \rightarrow {}^5G_2$, $^7F_0 \rightarrow {}^5L_6$ and $^7F_0 \rightarrow {}^5D_2$ under the 613 nm monitoring. According to Jorgensen's equation, the charge transfer band (CTB) position from the 2p orbital of O^{2-} to the 4*f* orbital of Eu^{3+} is estimated around 250 nm [26]. However, it does not appear obviously in the excitation spectrum, so the board bands in the UV region may contain the CTB of O^{2-}–Eu^{3+} and the energy transfer transition from tungstate groups to Eu^{3+} ions, and it is difficult to distinguish these two components due to spectral overlapping [23,27].

As shown in Fig. 3 (lines c and d), under the LMCT excitation at 282 nm, the PL spectrum of $ZnWO_4$ host lattice exhibits a broad blue-green emission band ranging from 380 to 580 nm with peak wavelength at 466 nm, which is assigned to the $O^{2-} \rightarrow W^{6+}$ LMCT states. After Eu^{3+} is introduced into the host lattice, it can be seen clearly not only the broad emission of tungstate groups but also the characteristic red emission of Eu^{3+} at 577, 590, 613 and 624 nm correspond to $^5D_0 \rightarrow {}^7F_J$ (J = 0–3) transitions, respectively. Among these narrow emission bands, the $^5D_0 \rightarrow {}^7F_2$ emission is dominating. The optimized Eu content value for the $^5D_0 \rightarrow {}^7F_2$ red emission is 3%, i.e., $ZnWO_4$:3% Eu^{3+} phosphors. In principle, Eu^{3+} is a good probe for the crystal field environment of the rare earth ions, because the $^5D_0 \rightarrow {}^7F_2$ transition (allowed by electric dipole) is very sensitive to the surroundings environment, while the $^5D_0 \rightarrow {}^7F_1$ transition (allowed by magnetic dipole) is insensitive to the environment. When Eu^{3+} located in a site with inversion symmetry, the $^5D_0 \rightarrow {}^7F_1$ transition is dominating. Conversely, the $^5D_0 \rightarrow {}^7F_2$ transition is dominating in an asymmetric site [28,29]. Therefore, it can be deduced that Eu^{3+} ions occupy the lattice sites without inversion symmetry in $ZnWO_4$ host lattice. In addition, it is shown that the emission intensity caused by tungstate group reduced compared to the undoped sample, indicating an efficient energy transfer from tungstate group to Eu^{3+} [27]. Moreover, the emission from higher Eu^{3+} excited states ^5D_J (J = 1–3) is absent, which may be ascribed to two possibilities. The emission from the higher levels ^5D_J may be generally quenched by multiphonon relaxation or overlapped by the broadband of O → W transition [30,31], and it is hard to say which one is the dominant factor for the absence of the ^5D_J emission.

To investigate the dependence of the visible emission color and intensity on the Eu^{3+} doping-concentration, Fig. 4 presents a series PL spectra of $ZnWO_4$:$x$$Eu^{3+}$ (x = 0, 0.1, 0.5, 1, 2, 3, 5 mol.%) nanorods prepared at pH = 6 with the reaction temperature of 180 °C. It can be seen clearly that the emission intensity of blue-green band decreases gradually with increasing Eu^{3+} concentration from 0 to 3 mol.%. Meanwhile, the emission intensity of Eu^{3+} exhibits the opposite tendency, which confirms the efficient energy transfer process from WO_4^{2-} to Eu^{3+}. However, the emission intensity of

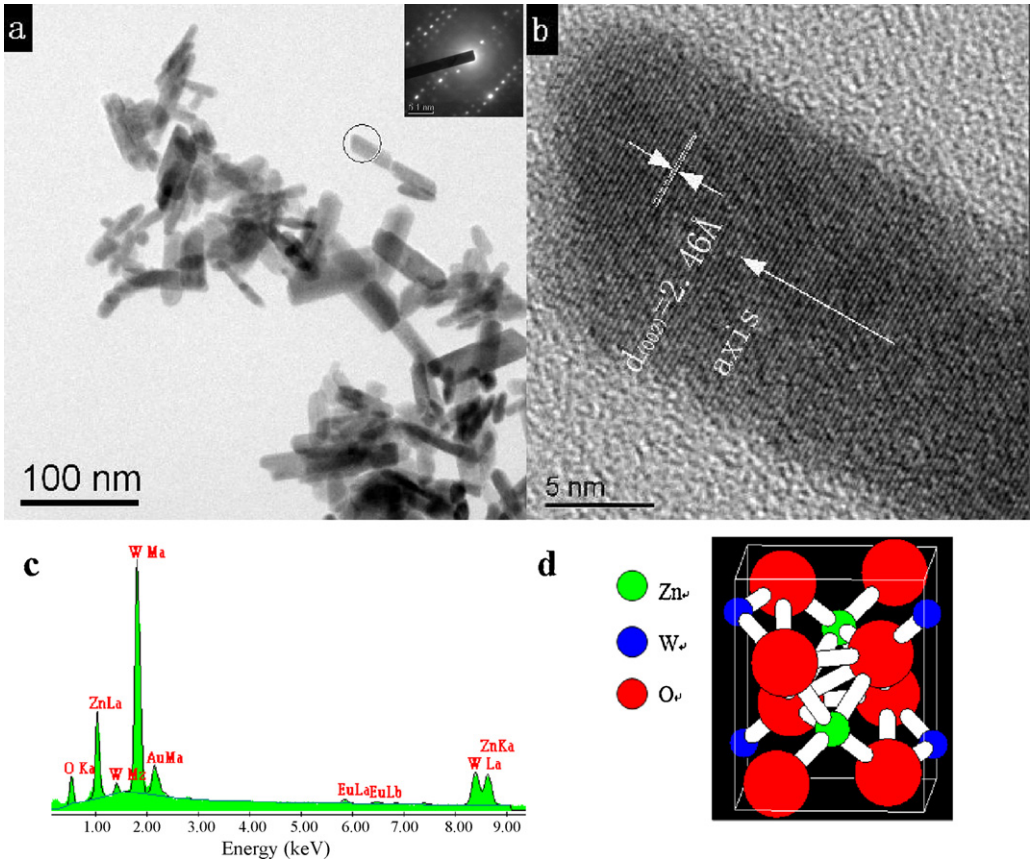

Fig. 2. (a) Transmission electron microscopy (TEM) image of $ZnWO_4$:5% Eu^{3+} synthesized in pH = 6, inset shows the selected-area electron diffraction (SADE) pattern for a single nanorod. (b) High resolution TEM (HRTEM) image of the corresponding single nanorod, (c) energy dispersive spectrometry (EDS) pattern of $ZnWO_4$:5% Eu^{3+}, and (d) the schematic diagram of crystal structure for $ZnWO_4$.

tungstate group increases and Eu^{3+} decreases again when the concentration of Eu^{3+} reaches 5%, due to concentration quenching [27].

The inset of Fig. 4 shows the decay curves of both the $ZnWO_4$ and $ZnWO_4$:0.1% Eu^{3+} nanorods, respectively. The decay curves for 466 nm emission (λ_{ex} = 282 nm) can approximatively fit into a single-exponential formula $I(t) = I(0)\exp(-t/\tau)$ [32], where $I(0)$ is the initial emission intensity and τ represents the $1/e$ lifetime of the emission center. The lifetime is determined to be 17.5 and 15.4 μs for $ZnWO_4$ and $ZnWO_4$:0.1% Eu^{3+} nanorods, respectively. The shortening lifetime of $ZnWO_4$:0.1% Eu^{3+} is a further evidence for the energy transfer from WO_4^{2-} to Eu^{3+} in $ZnWO_4$ host.

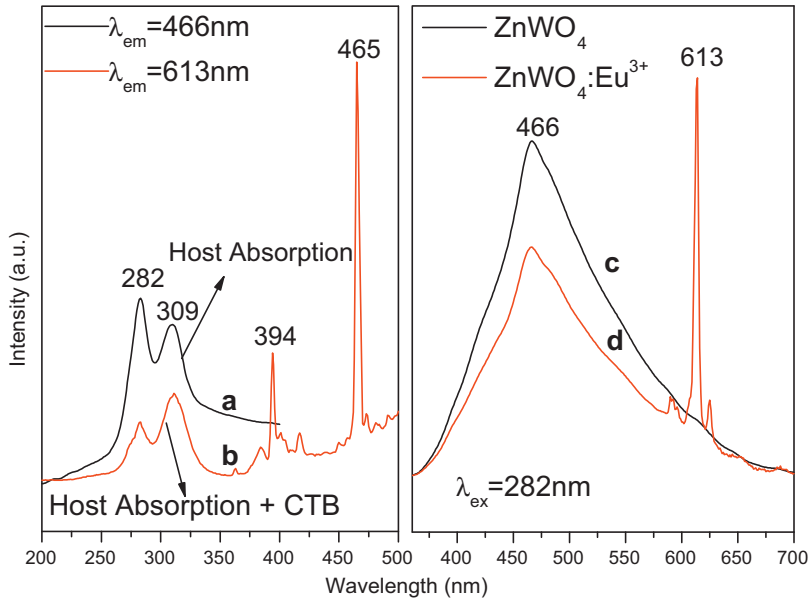

Fig. 3. PLE spectra of (a) $ZnWO_4$ host lattice (λ_{em} = 466 nm) and (b) $ZnWO_4$:5% Eu^{3+} (λ_{em} = 613 nm) (left); PL spectra of (c) $ZnWO_4$ host lattice and (d) $ZnWO_4$:5% Eu^{3+} (λ_{ex} = 282 nm) (right).

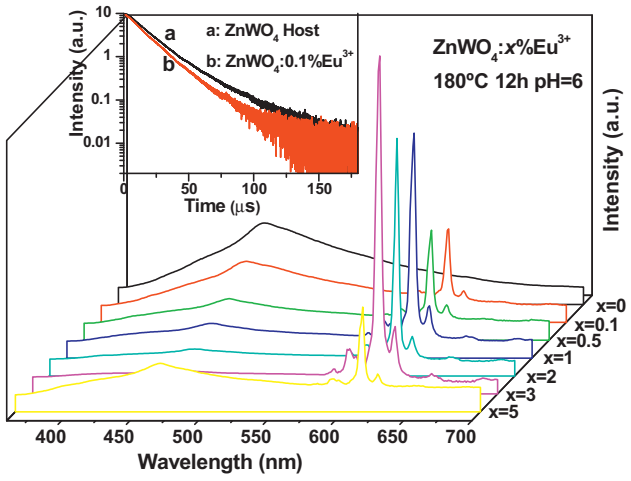

Fig. 4. PL spectra of $ZnWO_4$:xEu^{3+} (mol.%) (x = 0, 0.1, 0.5, 1, 2, 3, 5) (λ_{ex} = 282 nm). Inset shows the luminescence decay curves of WO_4^{2-} in (a) $ZnWO_4$, (b) $ZnWO_4$:0.1% Eu^{3+} (λ_{ex} = 282 nm).

Fig. 5 illustrates the model of the possible PL process with principal radiative and nonradiative courses. Upon excitation at 282 nm, the charge transfer of $O^{2-} \rightarrow W^{6+}$ firstly happens and emits blue-green light extending from 380 to 580 nm. On the other hand, efficient energy transfer from WO_4^{2-} to 4*f* shell of Eu^{3+} occurs. Thus, the electrons of Eu^{3+} at $^5D_0$ excited state can populate both from the nonradiative charge transfer feeding and the $^5D_J \rightarrow {}^5D_0$ relaxation, then emit the characteristic red light at 577, 590, 613 and 624 nm corresponding to the $^5D_0 \rightarrow {}^7F_J$ (J = 0–3) transitions, respectively.

Following the available CIE (Commission International de L'Eclairage, France, 1931) standard, we computed the CIE chromaticity coordinates (x, y) of $ZnWO_4$:Eu^{3+} phosphors and are marked as points a, b, c, d, e, f and g in Fig. 6. In the figure, R, G, and B (denoted by black squares) represent the color gamut positions of red, green, and blue of CRTs, respectively, i.e., R for Y_2O_2S:Eu (x = 0.624, y = 0.337), G for ZnS:Cu,Al (x = 0.312, y = 0.597), and B for ZnS:Ag (x = 0.157, y = 0.069) [33]. The upper arc in Fig. 6 is the locus of saturated colors. All the colors and shades that eye can

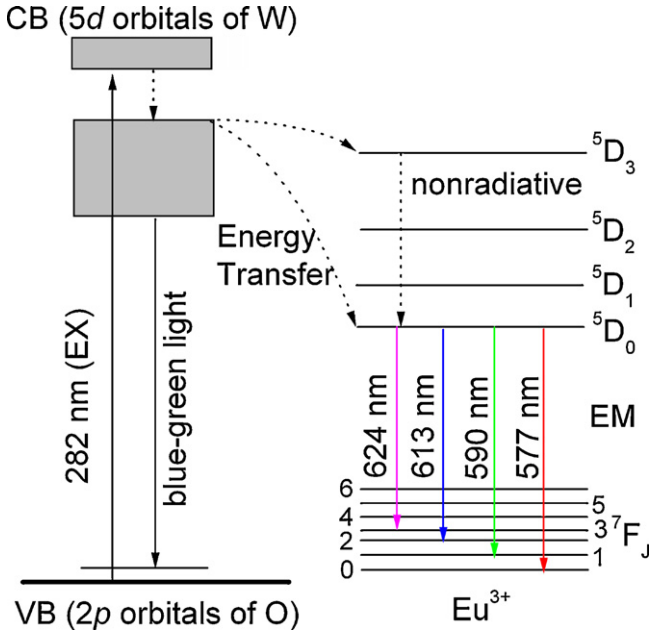

Fig. 5. The schematic energy level diagrams of possible excitation and visible emission for $ZnWO_4$:Eu^{3+} system.

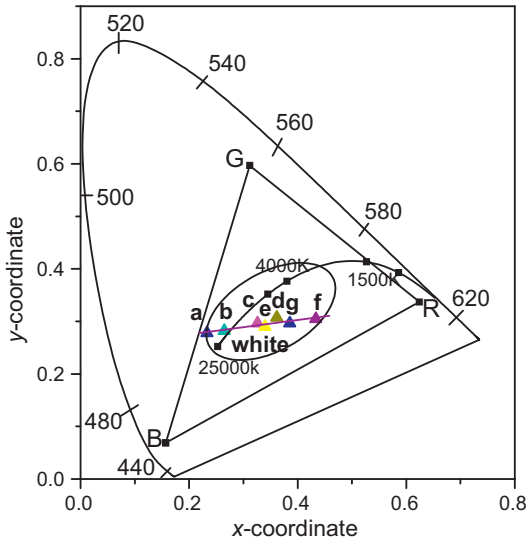

Fig. 6. The corresponding CIE chromaticity diagram of $ZnWO_4$:x% Eu^{3+} (mol.%) with various Eu^{3+} concentrations (G, R, B: CRTs coordinates), (a) x = 0, (b) x = 0.1, (c) x = 0.5, (d) x = 1, (e) x = 2, (f) x = 3, (g) x = 5.

resolve are enclosed between the area of saturated colors and the straight line labeled magenta. The central region appears white. The corresponding CIE coordinates for $ZnWO_4$:xEu^{3+} (x = 0, 0.1, 0.5, 1, 2, 3, 5 mol.%) phosphors are determined to be (x = 0.23, y = 0.24), (x = 0.27, y = 0.29), (x = 0.32, y = 0.30), (x = 0.40, y = 0.30), (x = 0.42, y = 0.31), (x = 0.50, y = 0.32) and (x = 0.31, y = 0.29), respectively. As shown in Fig. 6, the color tone changes from blue (represented by point a) through white zone (represented by points b, c, d, e) and finally to orange (represented by point f) with increasing concentration of Eu^{3+} ion. Especially, the point c (x = 0.5) which locates at x = 0.32, y = 0.30 with a color temperature of 5919 K, is very close to the standard white chromaticity (x = 0.33, y = 0.33) for the National Television Standard Committee (NTSC) system. In summary, a fine-tuning emission color can be easily realized by adjusting the Eu^{3+} concentration appropriately in a single-phased host lattice.

4. Conclusions

In summary, we briefly concluded that $ZnWO_4$:x% Eu^{3+} $0 \leq x \leq 5$ nanorods were prepared by a facile template-free hydrothermal route. Upon excitation at 282 nm, white light emission was obtained by combining the blue-green emission assigned to the charge-transfer transition of tungstate group and the red emissions of Eu^{3+}. Investigation of the variation concentration of Eu^{3+} indicated the energy transfer from tungstate group to Eu^{3+} in $ZnWO_4$ host. Tunable color from blue though white and finally to orange could be realized by adjusting the Eu^{3+}-doping concentration. A nearly ideal white light of $ZnWO_4$:0.5% Eu^{3+} with CIE coordinates (x = 0.32, y = 0.30) and color temperature of 5919 K implies the potential applications in deep ultraviolet LEDs for pc-WLEDs.

Acknowledgements

This work is joint supported by the NSFC (Grant No. 50872036) and the Fundamental Research Funds for the Central Universities, SCUT.

References

[1] D.P. Dutta, R. Ghildiyal, A.K. Tyagi, J. Phys. Chem. C 113 (2009) 16954.
[2] G.G. Li, C. Peng, C.X. Li, P.P. Yang, Z.Y. Hou, Y. Fan, Z.Y. Cheng, J. Lin, Inorg. Chem. 49 (2010) 1449.

[3] L.D. Carlos, R.A.S. Ferreira, V.Z. Bermudez, S.J.L. Ribeiro, Adv. Mater. 21 (2009) 509.
[4] H.W. Song, L.X. Yu, S.Z. Lu, T. Wang, Z.X. Liu, L.M. Yang, Appl. Phys. Lett. 85 (2004) 470.
[5] V. Bedekar, P.D. Dutta, M. Mohapatra, S.V. Godbole, R. Ghildiyal, A.K. Tyagi, Nanotechnology 20 (2009) 125707.
[6] P. Schlotter, R. Schmidt, J. Schneider, Appl. Phys. A 64 (1997) 417.
[7] K. Toda, Y. Kawakami, S.I. Kousaka, Y. Ito, A. Komeno, K. Uematsu, M. Sato, IEICE Trans. Electron. E89–C 10 (2006) 1406.
[8] Y.Q. Li, A.C.A. Delsing, G. de With, H.T. Hintzen, Chem. Mater. 17 (2005) 3242.
[9] Y.C. Liao, C.H. Lin, S.L. Wang, J. Am. Chem. Soc. 127 (2005) 9986.
[10] C.H. Liang, Y.C. Chang, Y.S. Chang, Appl. Phys. Lett. 93 (2008) 211902.
[11] S. Ye, F. Xiao, Y.X. Pan, Q.Y. Zhang, Mater. Sci. Eng. R (2010), doi:10.1016/j.mser.2010.07.001.
[12] X.M. Liu, C.K. Lin, J. Lin, Appl. Phys. Lett. 90 (2007) 081904.
[13] J. Lin, Y.F. Zhu, Inorg. Chem. 46 (2007) 8372.
[14] X.C. Song, E. Yang, R. Ma, H.F. Chen, Z.L. Ye, M. Luo, Appl. Phys. A 94 (2009) 185.
[15] K. Mayes, A. Yasan, R. McClintock, D. Shiell, S.R. Darvish, P. Kung, M. Razeghia, Appl. Phys. Lett. 84 (2004) 1046.
[16] A.J. Fischer, A.A. Allerman, M.H. Crawford, K.H.A. Bogart, S.R. Lee, R.J. Kaplar, W.W. Chow, S.R. Kurtz, K.W. Fullmer, J.J. Figiel, Appl. Phys. Lett. 84 (2004) 3394.
[17] Z.L. Wang, H.L. Li, J.H. Hao, J. Electrochem. Soc. 155 (2008) J152.
[18] M. Bonanni, L. Spanhel, M. Lerch, E. Füglein, G. Müller, Chem. Mater. 10 (1998) 304.
[19] H.Y. He, Phys. Stat. Solidi B 246 (2009) 177.
[20] H. Li, R. Liu, R.X. Zhao, Y.F. Zheng, W.X. Chen, Z.D. Xu, Cryst. Growth Des. 6 (2006) 2795.
[21] S.H. Yu, B. Liu, M.S. Mo, J.H. Huang, X.M. Liu, Y.T. Qian, Adv. Funct. Mater. 13 (2003) 639.
[22] S.J. Chen, J.H. Zhou, X.T. Chen, J. Li, L.H. Li, J.M. Hong, Z.L. Xue, X.Z. You, Chem. Phys. Lett. 375 (2003) 185.
[23] Q.L. Dai, H.W. Song, X. Bai, G.H. Pan, S.Z. Lu, T. Wang, X.G. Ren, H.F. Zhao, J. Phys. Chem. C 111 (2007) 7586.
[24] D. Errandonea, F.J. Manjón, R.P. Garro, S. Radescu, A. Mujica, A. Muñoz, C.Y. Tu, Phys. Rev. B 78 (2008) 054116.
[25] Z.D. Lou, J.H. Hao, M. Cocivera, J. Lumin. 99 (2002) 349.
[26] Y.G. Su, L.P. Li, G.S. Li, Chem. Mater. 20 (2008) 6060.
[27] F.S. Wen, X. Zhao, H. Huo, J.S. Chen, E.S. Lin, J.H. Zhang, Mater. Lett. 55 (2002) 152.
[28] C.C. Torardi, C. Page, L.H. Brixner, J. Solid State Chem. 69 (1987) 171.
[29] L. Fang, Y. Bing, J. Phys. Chem. C 113 (2009) 1074.
[30] X.P. Fan, D.B. Pi, F. Wang, J.R. Qi, M.Q. Wang, IEEE Trans. Nanotechnol. 5 (2006) 123.
[31] R. Schmechel, M. Kennedy, H. Seggern, H. Winkler, M. Kolbe, R. Fischer, X. Li, A. Benker, M. Winterrer, H. Hahn, J. Appl. Phys. 89 (2001) 1679.
[32] Q.Y. Zhang, X.Y. Huang, Prog. Mater. Sci. 55 (2010) 353.
[33] Q.Y. Zhang, K. Pita, W. Ye, W.X. Que, Chem. Phys. Lett. 351 (2002) 163.